Nanoscale Horizons

ROYAL SOCIETY OF CHEMISTRY

COMMUNICATION

View Article Online
View Journal | View Issue

Cite this: *Nanoscale Horiz.*, 2025, **10**, 3041

Received 12th June 2025,
Accepted 28th August 2025

DOI: 10.1039/d5nh00412h

rsc.li/nanoscale-horizons

Pattern and precision: DNA-based mapping of spatial rules for T cell activation

Shujie Li, Kaltrina Paloja and Maartje M. C. Bastings *

The nanoscale spatial arrangement of T cell receptor (TCR) ligands critically influences their activation potential in CD8$^+$ T cells, yet a comprehensive understanding of the molecular landscape induced by engagement with native peptide-MHC class I (pMHC-I) remains incomplete. Using DNA origami nanomaterials, we precisely organize pMHC-I molecules into defined spatial configurations to systematically investigate the roles of valencies, inter-ligand spacings, geometric patterns, and molecular flexibility in regulating T cell function. We find that reducing the inter-ligand spacing to ~7.5 nm enhances T cell activation by up to eightfold compared to a wider spacing (~22.5 nm), and that as few as six pMHC-I molecules are sufficient to elicit a robust response. Notably, the geometry of pMHC-I presentation emerges as a key determinant of signaling strength, with hexagonal arrangements proving most effective. In contrast, the introduction of flexible linkers into pMHC-I impairs TCR triggering. Together, these findings define spatial parameters that govern pMHC-I–TCR interactions at the T cell interface and provide design principles for engineering next-generation T cell-based immunotherapies.

New concepts

This work introduces the concept of multivalent spatial engineering to define the nanoscale parameters that govern T cell activation by native peptide-MHC class I (pMHC-I) ligands. While previous studies have emphasized ligand density or used high-affinity antibody surrogates, we use DNA origami to independently control valencies, inter-ligand spacings, geometric patterns, and molecular rigidity, enabling a systematic and physiologically relevant analysis of TCR triggering. We demonstrate that not just the number, but the spatial symmetry and rigidity of ligands are critical for efficient activation, with hexagonally patterned, rigid pMHC-I clusters outperforming other configurations. This uncovers a spatial tolerance window for productive TCR–pMHC engagement, revealing that even nanometer-scale deviations in ligand positioning or flexibility impair signaling. Our findings shift the paradigm from conventional multivalency toward precision spatial design as a key determinant of immune function. This conceptual advance provides a foundation for engineering immunomodulatory materials with defined nanoscale architectures, offering new directions for nanomedicine, vaccine design, and cell-based immunotherapy.

Introduction

Cytotoxic T cell-mediated killing is a central mechanism for eliminating malignant cells and underpins the therapeutic success of adoptive T cell immunotherapy and immune checkpoint blockade.[1,2] Activation of naïve CD8$^+$ T cells begins with the engagement of the T cell receptor (TCR) by peptide-MHC class I (pMHC-I) complexes presented on the surface of antigen-presenting cells (APCs), such as dendritic cells (DCs).[3] This communication between T cells and DCs is orchestrated by a diverse array of immune receptors whose spatiotemporal organization at the immunological synapse critically shapes the strength and quality of the T cell response.[4] Upon recognition of pMHC on DCs, TCRs rapidly organize into nanoclusters at the center of the T cell–DC interface, typically containing 5–30 receptors within a 35–70 nm radius.[5] This nanoscale organization has been shown to play a key role in modulating TCR signaling and likely reflects the spatial constraints required for its ligands.[6–8] As such, understanding the precise nanoscale requirements of TCR ligands that govern TCR triggering and T cell activation is essential and holds promise for the rational design of immune-modulating materials. However, mapping this molecular landscape within the complex context of T cell immunity remains a major challenge, as it demands platforms capable of controlling ligand presentation with nanometer-level precision.

The combination of high programmability and site-specific addressability endows DNA nanotechnology with a unique ability to control the spatial distribution of molecular components with nanometer precision.[9–12] As a result, functional DNA origami has enabled new paradigms for probing immunoreceptor–ligand interactions and holds significant promise for

Programmable Biomaterials Laboratory, Institute of Materials, Interfaculty Bioengineering Institute, School of Engineering, Ecole Polytechnique Fédérale Lausanne, Lausanne, 1015, Switzerland. E-mail: maartje.bastings@epfl.ch

applications in cell-based immunotherapy.[13–18] Using DNA origami to present TCR-stimulating ligands such as anti-CD3ε antibodies (aCD3ε), previous studies have shown that $CD8^+$ T cell activation reaches a plateau when three aCD3ε molecules are displayed, and increases as the inter-ligand spacing is reduced from 95 nm to 16 nm.[19] Similarly, in chimeric antigen receptor (CAR) T cell systems, optimal activation was achieved with four high-affinity DNA ligands arranged on DNA origami nanogrids, whereas further increasing ligand density resulted in premature termination of TCR signaling.[20] These findings, based on high-affinity TCR surrogates, provide valuable insights into the spatial constraints required for productive T cell activation. However, TCR triggering by high-affinity antibodies differs fundamentally from activation *via* the native ligand, pMHC.[21–24] As such, using pMHC offers a physiologically relevant platform for dissecting the spatial parameters underlying the local molecular landscape TCR activation.

More recently, the functional impact of pMHC spatial organization was investigated by manipulating two key parameters using DNA origami nanoscaffolds: density and inter-ligand spacing. Notably, densely clustered pMHC assemblies containing at least six streptavidin (SA) binding sites elicited stronger $CD8^+$ T cell activation compared to free pMHC, with closer proximity between ligands correlating with enhanced activation.[25] While these findings underscore the importance of multivalent pMHC arrangement, the study did not fully disentangle the individual contributions of valencies and density, as the inter-ligand spacing was not uniformly controlled across different DNA origami designs. Additionally, pMHC clustering on triangular DNA origami was achieved through biotin–streptavidin interactions, where each tetravalent SA molecule could bind up to three biotinylated pMHC ligands.[26] This inherent multivalency complicates precise interpretation of how individual pMHC molecules contribute to T cell activation and obscure accurate measurement of true inter-ligand spacing.

While increasing attention has been paid to ligand valencies and inter-ligand spacings, the importance of local geometric patterns remains underexplored in the context of immune activation. We have previously shown that the geometric arrangement of multivalent ligands can critically determine the onset of superselective receptor binding,[27] a phenomenon particularly relevant in the immune system, where ligand–receptor interactions are tightly regulated to preserve functional specificity and avoid aberrant activation.[28] Indeed, CD95L arranged in a hexagonal pattern with 10 nm spacing on DNA origami was found to strongly induce CD95-mediated apoptotic signaling in activated immune cells, aligning precisely with the topography of CD95 receptor clusters on the cell surface.[29,30] Similarly, IgG antibodies have been shown to efficiently activate the complement system through ordered clustering into hexamers.[31] Moreover, the spatial patterning of PD-1 has been reported to influence its interaction with PD-L1 on dendritic cells, further supporting geometric organization as a key determinant of receptor engagement.[32] Beyond patterning, the local flexibility of ligand linkers is another critical design variable. Maintaining rigidity is essential for discerning spatial effects on immune receptor triggering. This principle has been demonstrated in studies involving the B cell receptor, toll-like receptors, and Fas (CD95) signaling, where rigid presentation enhanced receptor activation.[33–36] Likewise, effector $CD4^+$ T cells produce more cytokines in response to increasingly rigid substrates presenting TCR ligands, suggesting that the mechanical properties of the interface also modulate downstream immune responses.[37] Despite growing interest, the combined impact of geometric patterns, rigidity, and linker flexibility on T cell signaling remains poorly characterized, representing a significant gap in our understanding of the spatial requirements for productive TCR triggering at the immunological synapse.

In this study, we systematically dissect how valencies, inter-ligand spacings, geometric patterns, and ligand rigidity of pMHC-I independently influence T cell activation. By maintaining a constant inter-ligand spacing, we first investigated the effect of varying pMHC-I valencies and found that multivalency linearly enhanced T cell activation at a spacing of ~15 nm. Reducing the inter-ligand distance to ~7.5 nm further amplified the response, with just six pMHC-I molecules sufficient to elicit robust T cell activation. We next explored the roles of geometric patterns and molecular flexibility, demonstrating that a compact hexagonal arrangement of pMHC-I elicited the strongest activation, while ligand flexibility impaired TCR signaling by disrupting the tight spatial constraints required for productive TCR–pMHC engagement. Together, our findings provide new insights into the nanoscale spatial requirements governing pMHC–TCR interactions and underscore the importance of precisely tailoring spatial parameters in the rational design of multivalent materials for T cell-based immunotherapies.

Results and discussion

Dense pMHC-I clusters reveal spatial threshold for efficient T cell stimulation

To investigate how TCR ligand valencies and inter-ligand spacings influence T cell activation, we used a two-layer, 60 nm diameter disk-shaped DNA origami nanoplatform.[38] This structure was strategically chosen to mimic the geometry of the immunological synapse and offers robust site-specific positioning of macromolecules[32,39] (Fig. S1). We generated a library of DNA disks presenting ovalbumin ($OVA_{257–264}$; SIINFEKL)-loaded MHC-I molecules (termed pMHC-I) with controlled valencies (0, 4, 6, 8, and 12) and inter-ligand spacings (7.5 nm or 15 nm), enabling a systematic evaluation of their individual and combined effects on the activation of primary $CD8^+$ T cells (Fig. 1a, b and Fig. S2, S3). At a 7.5 nm spacing, T cell activation increased with rising pMHC-I valencies from 0 to 6, confirming a positive correlation between the ligand number and TCR triggering as reported previously[25,40] (Fig. 1c). However, increasing the valency beyond six yielded minimal additional benefits in terms of activation markers CD69, CD25, and CD137, which represent early, late, and very late activation, respectively. While a slight resurgence in activation was observed at valency 12, this did not translate into increased cytotoxic function, as measured by expression of FasL (a death-inducing ligand) and CD107a (a marker of

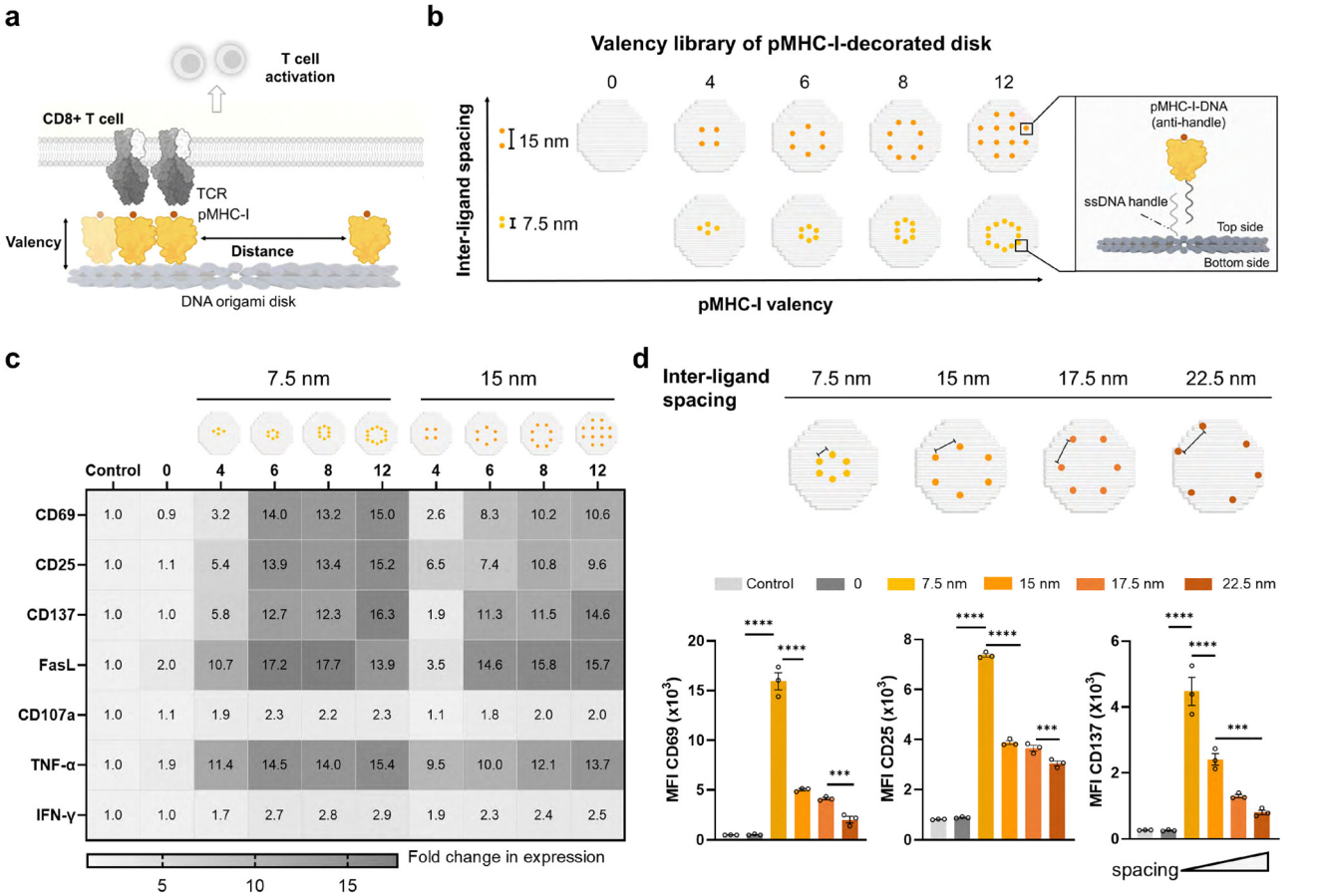

Fig. 1 Effects of pMHC-I valencies and inter-ligand spacings on CD8$^+$ T cell activation. (a) Schematic presentation of exploring the impact of clustering differences (valencies and inter-ligand spacings) of pMHC-I on CD8$^+$ T cell activation with a DNA origami disk nanoplatform, created partially with Biorender.com; (b) schematic presentation of the DNA origami disk designs used in the T cell activation assay. Engineered pMHC-I was decorated onto the DNA disk *via* handle-anti-handle hybridization; (c) flow cytometry analysis of biomarkers and cytokine expression in CD8$^+$ T cells following stimulation with DNA disks at 24 h (CD69), 48 h (CD25, TNF-α, IFN-γ), and 72 h (CD137, FasL, CD107a). Fold changes in expression are represented as the mean fluorescence intensity (MFI) values relative to the untreated control group ($n \geq 6$ from two independent experiments); and (d) MFI of CD69 (24 h), CD25 (48 h), and CD137 (72 h) in CD8$^+$ T cells stimulated by DNA origami presenting pMHC-I with varied inter-ligand spacing. Data are shown as mean ± SEM (n = 3 biological replicates). Statistical significance was assessed using one-way ANOVA with Tukey's multiple comparison test (***$p < 0.001$, ****$p < 0.0001$).

degranulation). Cytokine secretion levels, including TNF-α and IFN-γ, aligned with the surface marker data, further supporting this saturation effect (Fig. 1c). When the inter-ligand spacing was increased from 7.5 nm to 15 nm, T cell activation decreased across all valency conditions, although the extent varied. Notably, for six pMHC-I ligands, CD69 expression dropped sharply at the wider spacing, whereas constructs presenting four ligands showed a more modest decline. Interestingly, at a 15 nm spacing, the valency became the dominant determinant of T cell activation, with activation levels increasing approximately linearly from valency 0 to 12 (Fig. 1c). Control experiments demonstrated that T cell activation followed a similar trend in the absence of soluble anti-CD28, supporting previous findings that costimulatory ligands do not obscure the intrinsic spatial effects of pMHC-I-mediated TCR stimulation[25] (Fig. S4). This suggests that tight spatial organization is particularly important at lower ligand densities, while a higher valency can partially compensate for suboptimal spacing.

We hypothesized that further reducing the inter-ligand spacing, particularly when using the physiological TCR ligand pMHC, might enhance T cell activation by better matching native TCR spatial constraints. This hypothesis was supported by our data, which revealed a clear distance-dependent trend in T cell activation using pMHC-I disks at a fixed valency of six: 7.5 nm > 15 nm > 17.5 nm > 22.5 nm (Fig. 1d and Fig. S5, S6). These results suggest that tighter spatial organization of ligands facilitates more efficient TCR triggering. This finding is consistent with prior results showing that three aCD3 antibodies spaced at 16 nm can induce saturated T cell activation.[19] As antibodies engage with 2 binding epitopes, effectively 6 interactions in 8 nm distance are formed. The robust activation we observed with six pMHC-I molecules spaced at 7.5 nm indicates that this distance may approximate a lower functional limit for effective ligand spacing on synthetic platforms. Taken together, our results demonstrate that a minimal unit of six pMHC-I molecules arranged at 7.5 nm spacing is sufficient to

induce strong T cell activation. This finding highlights that a low copy number of locally clustered native ligands is enough to stimulate a potent T cell response.[41]

Hexagonal ligand patterning maximizes T cell activation

To investigate whether the spatial patterning of pMHC-I molecules influences T cell activation, we assembled DNA disks presenting six pMHC-I ligands arranged in hexagonal (Hex), triangular (Tri), linear (Lin), and parallel (Par) configurations. Based on the consensus from our previous experiments, the ligand copy number and inter-ligand spacing were fixed at six and 7.5 nm, respectively (Fig. 2a and Fig. S7a, b). Strikingly, we observed that the geometric pattern of pMHC-I had a significant impact on both $CD8^+$ T cell activation and cytotoxic function (Fig. 2b and Fig. S7c). In particular, the linear configuration resulted in substantially lower expression of activation markers CD69, CD25, and CD137, as well as effector molecules FasL and CD107a, compared to the other patterns (Fig. 2b and Fig. S7c). This reduction is likely due to the mismatch between the linear arrangement of ligands and the clustered distribution of TCRs on the T cell surface, which favors engagement by locally clustered ligands.[42,43]

DNA disks presenting pMHC-I in triangular and parallel patterns elicited comparable levels of T cell activation, suggesting that local clustering, regardless of a precise pattern, supports efficient TCR triggering. However, the hexagonal arrangement induced the strongest activation profile, with 58.5% $CD69^+$, 70.3% $CD25^+$, and 36% $CD137^+$ T cells, substantially higher than

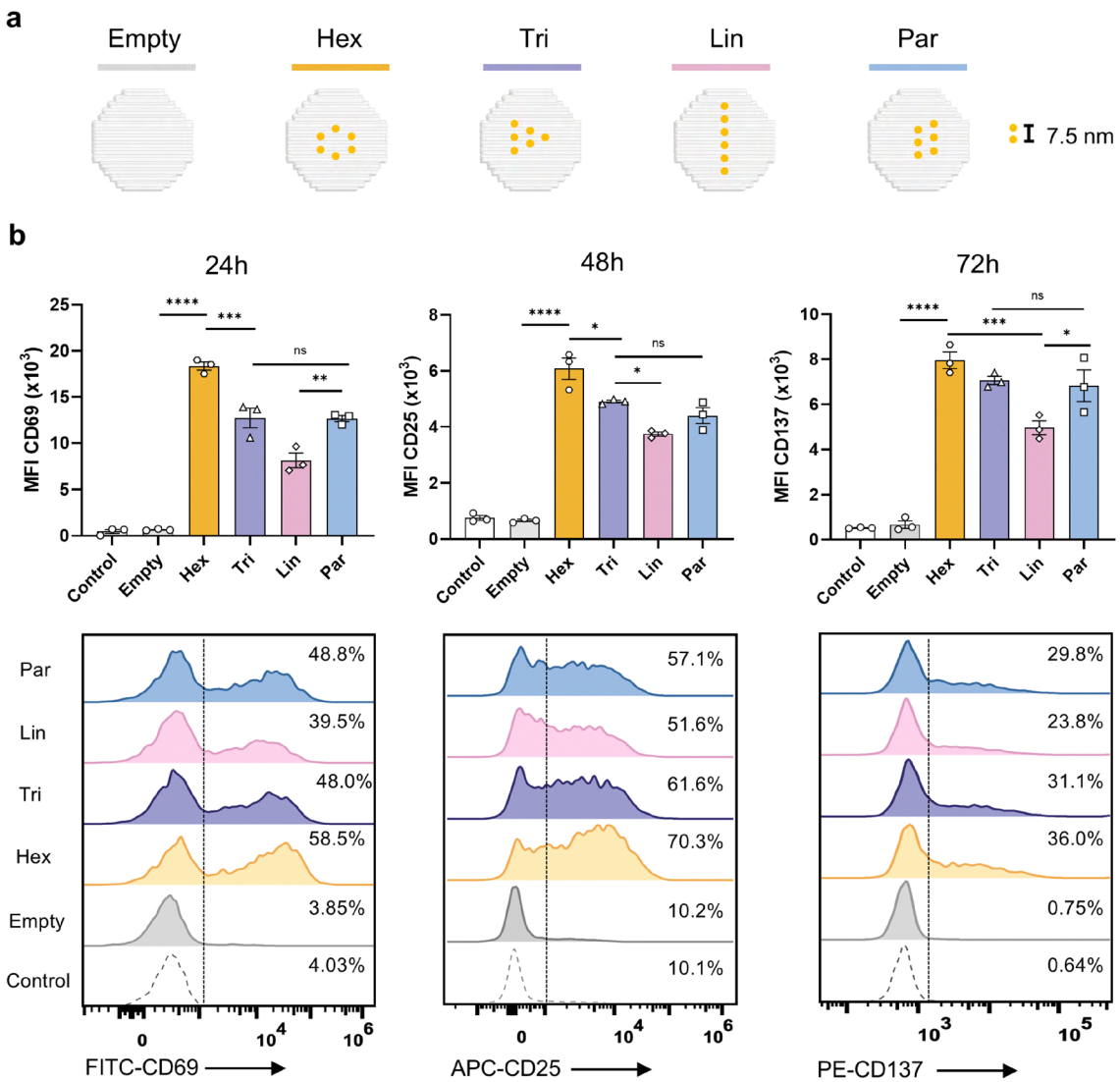

Fig. 2 Effects of the pMHC-I geometric pattern on $CD8^+$ T cell activation. (a) Schematic presentation of the DNA origami disk displaying pMHC-I in four different geometric patterns. Hex: hexagonal, Tri: triangular, Lin: linear, and Par: parallel. The inter-ligand spacing of pMHC-I was 7.5 nm. (b) Expression levels of CD69, CD25, and CD137 on $CD8^+$ T cells (upper panel) and representative flow cytometry data (lower panel) following stimulation with pMHC-I-patterned DNA disks, showing T cell activation at 24, 48, and 72 hours, respectively. Percentages of CD69+, CD25+, and CD137+ cells of each group were gated based on the untreated control group. Data are shown as mean ± SEM (n = 3 biological replicates). Statistical significance was assessed using one-way ANOVA with Tukey's multiple comparison test (*$p < 0.05$, **$p < 0.01$, ***$p < 0.001$, and ****$p < 0.0001$).

both the triangular and parallel configurations (Fig. 2b). One possible explanation is that the higher ligand density in the parallel and triangle patterns may cause steric hindrance, limiting full TCR engagement (Fig. S7d). Alternatively, the hexagonal arrangement, which has been reported to optimize antibody binding,[44] may provide greater geometric symmetry and multi-directional accessibility, thereby increasing the likelihood of TCR engagement, promoting stabilization of TCR nanoclusters, and facilitating the recruitment of downstream signaling molecules.

At the population level, the hexagonal configuration maximized the expression of all monitored biomarkers. The mean fluorescence intensity (MFI) for CD69 was 2.3-fold higher, and for CD25 and CD137 was 1.6-fold higher, compared to the linear pattern (Fig. 2b). Importantly, these measurements were obtained in live cells, where TCRs can laterally diffuse and reorganize. Despite this membrane fluidity, the pattern-dependent differences in activation remained robust and detectable. While previous studies have predominantly emphasized the role of ligand density in TCR triggering,[25] our findings highlight the critical and often overlooked role of geometric patterns, a spatial design parameter that may play a key role in natural immune cell–cell communication mediated by multivalent ligand–receptor interactions.

Flexibility compromises geometry-driven TCR triggering

Linker flexibility plays a key role in the design of functional nanomaterials by shaping the spatial interface through which ligands engage cell surface receptors. This parameter is especially critical in immune signaling, where the immunological synapse is both spatially and temporally confined. Prior studies have shown that immune synapse formation is most dynamic within the first 10 minutes of T cell–APC contact and remains detectable up to an hour later, indicating that TCR clusters exhibit constrained, directed motion during early activation.[45] This suggests that receptor engagement may require a certain degree of positional rigidity. In support of this, extending the linker length between pMHC dimers – thereby introducing flexibility – has been shown to disrupt TCR triggering.[46,47] Motivated by these insights, we examined the influence of ligand flexibility on $CD8^+$ T cell activation by modifying the rigidity of the DNA–pMHC-I interface. Specifically, we incorporated thymine (T) spacers into the ssDNA handle extending from the DNA disk, presenting pMHC-I ligands with increasing degrees of flexibility. We focused on the hexagonal (Hex_0T, Hex_5T, Hex_10T) and linear (Lin_0T, Lin_5T, Lin_10T) configurations, which previously showed the strongest and weakest activation potentials, respectively (Fig. 3a, c and Fig. S8a, b).

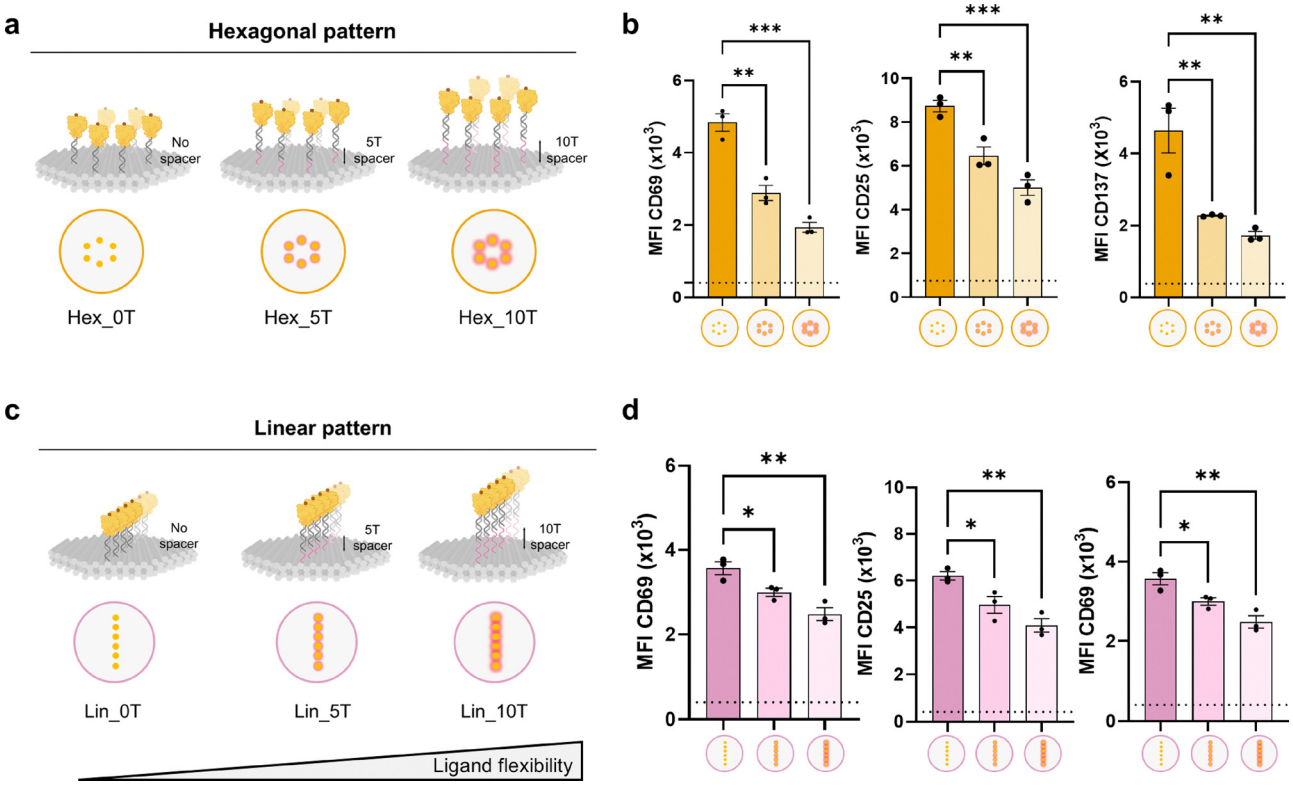

Fig. 3 Effects of pMHC-I ligand flexibility on $CD8^+$ T cell activation. (a) Schematic illustration of DNA origami disks presenting pMHC-I with increasing ligand flexibilities arranged in a hexagonal pattern, created partially with Biorender.com. (b) Expression levels of CD69 (24 h), CD25 (48 h), and CD137 (72 h) on $CD8^+$ T cells stimulated by hexagonally patterned pMHC-I DNA origami with varying ligand flexibilities. (c) Schematic illustration of DNA origami disks presenting pMHC-I with increasing ligand flexibilities arranged in a linear pattern, created partially with Biorender.com. (d) Expression levels of CD69 (24 h), CD25 (48 h), and CD137 (72 h) on $CD8^+$ T cells stimulated by linearly patterned pMHC-I DNA origami with varying ligand flexibilities. The dashed line indicates the corresponding biomarker expression induced by the empty DNA origami disk without pMHC-I decoration. Data are shown as mean ± SEM (n = 3 biological replicates). Statistical significance was assessed using one-way ANOVA with Tukey's multiple comparison test (*$p < 0.05$, **$p < 0.01$, ***$p < 0.001$).

Interestingly, the rigid Hex_0T configuration elicited significantly higher expression of activation markers CD69, CD25, and CD137 at both early and late time points compared to its more flexible counterparts (Hex_5T and Hex_10T) (Fig. 3b and Fig. S8c). T cell activation was progressively dampened as linker flexibility increased, with a consistent trend observed across both hexagonal and linear patterns (Fig. 3b, d and Fig. S8d), indicating a negative correlation between ligand flexibility and T cell activation. Importantly, the geometric pattern effect remained evident: hexagonal configurations consistently outperformed linear ones in stimulating T cells. However, the magnitude of this difference diminished with increasing linker flexibility, suggesting that the mechanical instability introduced by flexible linkers compromises the benefits of geometric presentation (Fig. S9). Similar trends were also observed for the parallel configuration, reinforcing the general principle that rigidity enhances TCR triggering across diverse spatial patterns (Fig. S10).

Mechanistic insight into ligand flexibility and spatial tolerance

To more precisely understand how ligand flexibility modulates T cell activation, we examined the underlying mechanisms involved. Previous studies have shown that spatial tolerance, a combination of ligand rigidity and matched receptor spacing, is essential for functional interactions, such as CpG–TLR9 binding.[35] In our system, introducing 5T or 10T single-stranded DNA spacers into the ligand handle increases positional uncertainty by approximately ±1.7 nm or ±3.4 nm, respectively, assuming full extension (Fig. 4a). This spatial deviation likely impairs the alignment between pMHC-I and TCR, as reflected by the diminished T cell activation observed with more flexible constructs (Fig. 3). Given that T cell activation is initiated *via* TCR–pMHC engagement, which in turn activates a tyrosine kinase cascade, we hypothesized that ligand flexibility disrupts early TCR signaling. During TCR activation, tyrosine kinase Lck phosphorylates CD3 subunit immunoreceptor tyrosine-based activation motifs (ITAM).[48,49] This recruits the protein tyrosine kinase ZAP-70 to initiate downstream signaling pathways such as the mitogen-activated protein kinase (MAPK), leading to phosphorylation of extracellular signal-regulated kinase ERK and activation of NF-κB, which regulates gene expression essential for T cell activation.[50,51] To test this, we monitored phosphorylation levels of ZAP70, ERK1/2, and NF-κB (p65), 15 minutes after stimulation. As expected, stimulation with non-functionalized DNA disks did not induce signaling above background levels seen in unstimulated $CD8^+$ T cells (Fig. 4b), enabling a clear assessment of the effects of ligand flexibility. Consistent with activation marker expression, the highest phosphorylation levels of ZAP70, ERK1/2, and NF-κB were observed in cells treated with rigid pMHC-I ligands (0T spacers), regardless of the geometric pattern (hexagonal or linear) (Fig. 4b). Intermediate signaling was observed for 5T constructs, while the 10T variants showed the weakest phosphorylation, further confirming that ligand flexibility negatively impacts TCR signaling efficiency.

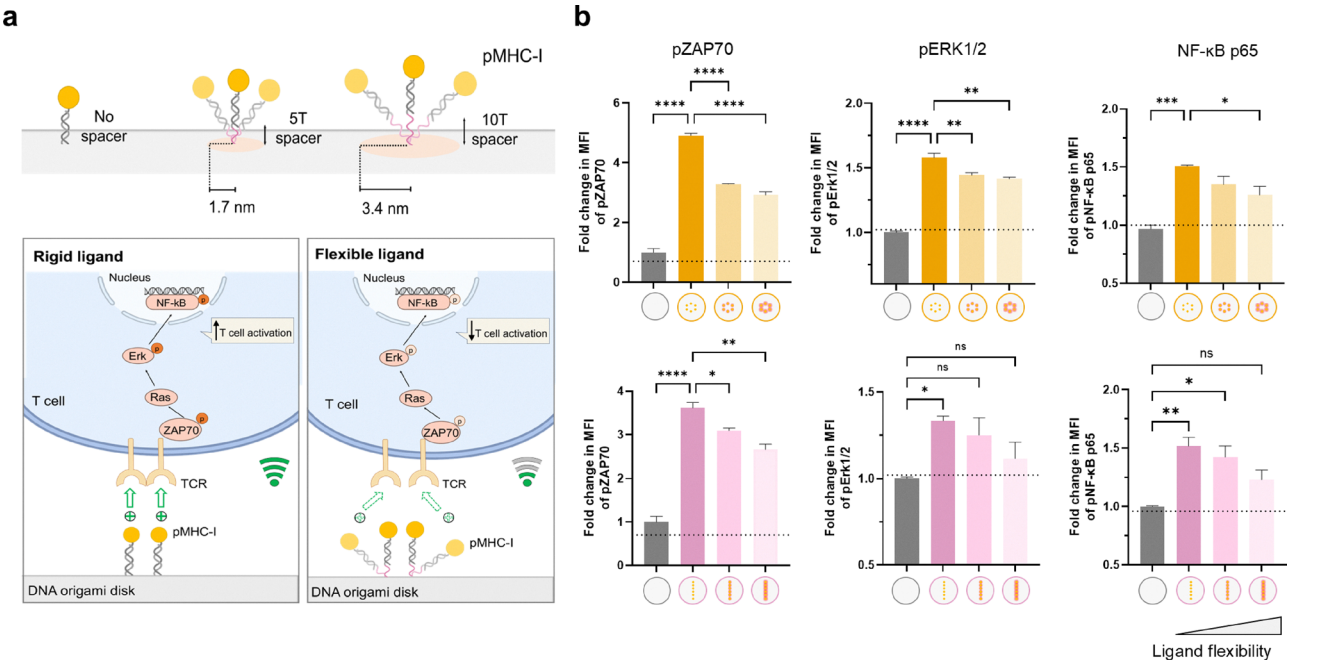

Fig. 4 Effects of pMHC-I ligand flexibility on TCR triggering. (a) Schematic representation of the estimated spatial deviations in pMHC-I positioning induced by 5T or 10T linkers (upper panel), and the corresponding TCR signal transduction triggered by rigid *versus* flexible pMHC-I ligands (lower panel), created partially with Biorender.com. (b) Relative MFI of phosphorylated ZAP70, ERK1/2, and NF-κB (p65) after 15 min stimulation with pMHC-I arranged in hexagonal (upper panel) or linear (lower panel) patterns on the DNA origami disk, with varying ligand flexibility. Data were normalized to the response from empty DNA origami without pMHC-I decoration. The dashed line indicates the protein phosphorylation level in unstimulated $CD8^+$ T cells. Data are shown as mean ± SEM (n = 3 biological replicates). Statistical significance was assessed using one-way ANOVA with Tukey's multiple comparison test (*$p < 0.05$, **$p < 0.01$, ***$p < 0.001$, ****$p < 0.001$).

Stronger signaling events were also observed with Hex_0T compared to Lin_0T (Fig. S11). While the TCR–CD3 complex serves as a basic signaling unit, co-receptors and adhesion molecules also constitute elements of TCR stimulation in the immune synapse,[52,53] suggesting that the precise mechanisms underlying the pattern effect on TCR signaling warrant further investigation.

We conclude that increased ligand flexibility disrupts the nanoscale coordination between pMHC-I and TCRs by introducing spatial deviations that reduce the frequency of productive short-distance TCR–pMHC interactions. To validate this, we compared flexible ligands (Hex_5T, Hex_10T) to rigid pMHC-I ligands spaced at 15 nm and 22.5 nm, respectively. As shown in Fig. S12, the activation potency of flexible ligands fell between the responses induced at 7.5 nm and 15 nm spacings, consistent with predicted effects of spatial mismatch. Importantly, TCR triggering is highly sensitive to spatial perturbations at the immune synapse, not only because of the ligand–receptor geometry but also due to the biophysical organization of the signaling interface. According to the kinetic segregation model, TCR signaling is initiated when close-contact zones between the T cell and antigen-presenting cell exclude large membrane phosphatases such as CD45, whose bulky extracellular domain ($\sim$50 nm) sterically prevents access to regions where the membranes are tightly apposed.[54–56] This exclusion allows kinases to phosphorylate ITAM motifs in the CD3 complex, thereby initiating downstream signaling. Extending the distance between APC and T cell membranes to 29 nm was previously reported to attenuate T cell signaling, likely due to impaired CD45 exclusion.[57] Given that the axial dimension at the T cell–DNA disk interface is estimated to be $<$20 nm (the TCR–pMHC pair creates a $\sim$13 nm contact[57,58]), and that the extra distance due to the T-spacers is $<$3 nm (Fig. S13), we consider no vital changes toward the accessibility of CD45. Taken together, our results reveal a spatial tolerance window for productive TCR triggering, demonstrating that even nanometer-scale deviations in ligand positioning, whether from increased spacing or flexibility, can significantly affect immune signaling. These findings underscore the extreme spatial sensitivity of the TCR–pMHC interface and reinforce the need for rigid, geometry-controlled presentation of ligands in the design of immunomodulatory materials.

Conclusion

While extensive efforts have been directed toward developing immune-engineering biomaterials to support T cell expansion and adoptive cell therapies, a comprehensive understanding of how the spatial presentation of TCR ligands governs T cell activation remains limited. Leveraging the unparalleled spatial precision of DNA nanotechnology, we systematically dissected the functional impacts of four key parameters of native TCR ligand (pMHC-I) presentation: valencies, inter-ligand spacings, geometric patterns, and ligand rigidity. By monitoring $CD8^+$ T cell responses, we found that a short inter-ligand spacing (7.5 nm) substantially enhances activation, and that as few as six pMHC-I molecules, when locally clustered, are sufficient to trigger a robust response. Notably, we show that ligand geometries play a decisive role: hexagonally arranged pMHC-I outperforms linearly arranged ligands of the identical valency, highlighting the importance of matching ligand spatial organization to receptor topology on the T cell surface. Furthermore, we demonstrate that ligand flexibility impairs TCR engagement and signaling, likely by disrupting the membrane proximity and nanoscale clustering required for the productive TCR–pMHC interaction and CD45 exclusion.

Together, these findings emphasize that effective multivalent interactions rely not only on ligand density, but on the precise engineering of spatial parameters including pattern symmetry and mechanical stability. This represents a conceptual shift from conventional multivalent binding to what we define as multivalent engineering: the deliberate spatial programming of ligand organization to engage biological interfaces with maximal functional control. In summary, our study delineates the spatial principles governing receptor–ligand interactions at the T cell interface and establishes a framework for the rational design of immunotherapeutic materials. By tuning the valencies, spacings, patterns, and rigidity, multivalent systems can be tailored to more effectively coordinate receptor engagement and downstream signaling, paving the way toward next-generation materials for T cell-based immunotherapy.

Author contributions

SL: investigation, data curation, conceptualization, methodology, formal analysis, project administration, writing original draft, and review and editing. KP: investigation and methodology. MMCB: conceptualization, supervision, project administration, funding acquisition, and writing review and editing.

Conflicts of interest

There are no conflicts to declare.

Data availability

The authors declare that all data supporting the findings of this study are available within the article and its SI. See DOI: **https://doi.org/10.1039/d5nh00412h**.

Any other data that support the findings of this study are available from the corresponding author upon reasonable request.

Acknowledgements

This work was funded by the Swiss Cancer League (grant KFS-5935-08-2023). We are grateful for the Protein Production and Structure Core Facility (PTPSP, EPFL) and the Flow Cytometry Core Facility (FCCF, EPFL) for instrument accessibility and operational support, and the Center of PhenoGenomics (CPG, EPFL) for housing the animals. The authors thank Yameng Lou and Dr Vincenzo Caroprese for their insightful discussions.

References

1 B. Weigelin and P. Friedl, T Cell-Mediated Additive Cytotoxicity – Death by Multiple Bullets, *Trends Cancer*, 2022, **8**(12), 980–987, DOI: **10.1016/j.trecan.2022.07.007**.

2 M. Morotti, A. Albukhari, A. Alsaadi, M. Artibani, J. D. Brenton, S. M. Curbishley, T. Dong, M. L. Dustin, Z. Hu, N. McGranahan, M. L. Miller, L. Santana-Gonzalez, L. W. Seymour, T. Shi, P. Van Loo, C. Yau, H. White, N. Wietek, D. N. Church, D. C. Wedge and A. A. Ahmed, Promises and Challenges of Adoptive T-Cell Therapies for Solid Tumours, *Br. J. Cancer*, 2021, **124**(11), 1759–1776, DOI: **10.1038/s41416-021-01353-6**.

3 J.-R. Hwang, Y. Byeon, D. Kim and S.-G. Park, Recent Insights of T Cell Receptor-Mediated Signaling Pathways for T Cell Activation and Development, *Exp. Mol. Med.*, 2020, **52**(5), 750–761, DOI: **10.1038/s12276-020-0435-8**.

4 S. Schafer, K. Chen and L. Ma, Crosstalking with Dendritic Cells: A Path to Engineer Advanced T Cell Immunotherapy, *Front. Syst. Biol.*, 2024, 4, DOI: **10.3389/fsysb.2024.1372995**.

5 B. F. Lillemeier, M. A. Mörtelmaier, M. B. Forstner, J. B. Huppa, J. T. Groves and M. M. Davis, TCR and Lat Are Expressed on Separate Protein Islands on T Cell Membranes and Concatenate during Activation, *Nat. Immunol.*, 2010, **11**(1), 90–96, DOI: **10.1038/ni.1832**.

6 F. Giannoni, J. Barnett, K. Bi, R. Samodal, P. Lanza, P. Marchese, R. Billetta, R. Vita, M. R. Klein, B. Prakken, W. W. Kwok, E. Sercarz, A. Altman and S. Albani, Clustering of T Cell Ligands on Artificial APC Membranes Influences T Cell Activation and Protein Kinase Cθ Translocation to the T Cell Plasma Membrane1, *J. Immunol.*, 2005, **174**(6), 3204–3211, DOI: **10.4049/jimmunol.174.6.3204**.

7 S. V. Pageon, T. Tabarin, Y. Yamamoto, Y. Ma, P. R. Nicovich, J. S. Bridgeman, A. Cohnen, C. Benzing, Y. Gao, M. D. Crowther, K. Tungatt, G. Dolton, A. K. Sewell, D. A. Price, O. Acuto, R. G. Parton, J. J. Gooding, J. Rossy, J. Rossjohn and K. Gaus, Functional Role of T-Cell Receptor Nanoclusters in Signal Initiation and Antigen Discrimination, *Proc. Natl. Acad. Sci. U. S. A.*, 2016, **113**(37), E5454–E5463, DOI: **10.1073/pnas.1607436113**.

8 Y. Jung, I. Riven, S. W. Feigelson, E. Kartvelishvily, K. Tohya, M. Miyasaka, R. Alon and G. Haran, Three-Dimensional Localization of T-Cell Receptors in Relation to Microvilli Using a Combination of Superresolution Microscopies, *Proc. Natl. Acad. Sci. U. S. A.*, 2016, **113**(40), E5916–E5924, DOI: **10.1073/pnas.1605399113**.

9 P. W. K. Rothemund, Folding DNA to Create Nanoscale Shapes and Patterns, *Nature*, 2006, **440**(7082), 297–302, DOI: **10.1038/nature04586**.

10 N. C. Seeman and H. F. Sleiman, DNA Nanotechnology, *Nat. Rev. Mater.*, 2017, **3**(1), 1–23, DOI: **10.1038/natrevmats.2017.68**.

11 C. E. Castro, F. Kilchherr, D.-N. Kim, E. L. Shiao, T. Wauer, P. Wortmann, M. Bathe and H. Dietz, A Primer to Scaffolded DNA Origami, *Nat. Methods*, 2011, **8**(3), 221–229, DOI: **10.1038/nmeth.1570**.

12 P. Wang, T. A. Meyer, V. Pan, P. K. Dutta and Y. Ke, The Beauty and Utility of DNA Origami, *Chem*, 2017, **2**(3), 359–382, DOI: **10.1016/j.chempr.2017.02.009**.

13 G. A. Knappe, E.-C. Wamhoff and M. Bathe, Functionalizing DNA Origami to Investigate and Interact with Biological Systems, *Nat. Rev. Mater.*, 2023, **8**(2), 123–138, DOI: **10.1038/s41578-022-00517-x**.

14 Y. Hou and B. Treanor, DNA Origami: Interrogating the Nano-Landscape of Immune Receptor Activation, *Biophys. J.*, 2024, **123**(15), 2211–2223, DOI: **10.1016/j.bpj.2023.10.013**.

15 G. Li, C. Chen, Y. Li, B. Wang, J. Wen, M. Guo, M. Chen, X.-B. Zhang and G. Ke, DNA-Origami-Based Precise Molecule Assembly and Their Biological Applications, *Nano Lett.*, 2024, **24**(37), 11335–11348, DOI: **10.1021/acs.nanolett.4c03297**.

16 Y. Zeng, R. L. Nixon, W. Liu and R. Wang, The Applications of Functionalized DNA Nanostructures in Bioimaging and Cancer Therapy, *Biomaterials*, 2021, **268**, 120560, DOI: **10.1016/j.biomaterials.2020.120560**.

17 Y. Qu, F. Shen, Z. Zhang, Q. Wang, H. Huang, Y. Xu, Q. Li, X. Zhu and L. Sun, Applications of Functional DNA Materials in Immunomodulatory Therapy, *ACS Appl. Mater. Interfaces*, 2022, **14**(40), 45079–45095, DOI: **10.1021/acsami.2c13768**.

18 C. Y. Tseng, W. X. Wang, T. R. Douglas and L. Y. T. Chou, Engineering DNA Nanostructures to Manipulate Immune Receptor Signaling and Immune Cell Fates, *Adv. Healthc. Mater.*, 2022, **11**(4), 2101844, DOI: **10.1002/adhm.202101844**.

19 L. Sun, F. Shen, Z. Xiong, Y. Chao, C. Fan and Z. Liu, Nanoscale Precise Editing of Multiple Immune Stimulating Ligands on DNA Origami for T Cell Activation and Cell-Based Cancer Immunotherapy, *CCS Chem*, 2023, **6**(3), 719–732, DOI: **10.31635/ccschem.023.202302858**.

20 R. Dong, T. Aksel, W. Chan, R. N. Germain, R. D. Vale and S. M. Douglas, DNA Origami Patterning of Synthetic T Cell Receptors Reveals Spatial Control of the Sensitivity and Kinetics of Signal Activation, *Proc. Natl. Acad. Sci. U. S. A.*, 2021, **118**(40), e2109057118, DOI: **10.1073/pnas.2109057118**.

21 J. Hellmeier, R. Platzer, A. S. Eklund, T. Schlichthaerle, A. Karner, V. Motsch, M. C. Schneider, E. Kurz, V. Bamieh, M. Brameshuber, J. Preiner, R. Jungmann, H. Stockinger, G. J. Schütz, J. B. Huppa and E. Sevcsik, DNA Origami Demonstrate the Unique Stimulatory Power of Single pMHCs as T Cell Antigens, *Proc. Natl. Acad. Sci. U. S. A.*, 2021, **118**(4), e2016857118, DOI: **10.1073/pnas.2016857118**.

22 K. B. Wilhelm, A. Vissa and J. T. Groves, Differential Roles of Kinetic On- and off-Rates in T-Cell Receptor Signal Integration Revealed with a Modified Fab'-DNA Ligand, *Proc. Natl. Acad. Sci.*, 2024, **121**(39), e2406680121, DOI: **10.1073/pnas.2406680121**.

23 M. A. Al-Aghbar, Y.-S. Chu, B.-M. Chen and S. R. Roffler, High-Affinity Ligands Can Trigger T Cell Receptor Signaling Without CD45 Segregation, *Front. Immunol.*, 2018, 9, DOI: **10.3389/fimmu.2018.00713**.

24 J. R. James and R. D. Vale, Biophysical Mechanism of T-Cell Receptor Triggering in a Reconstituted System, *Nature*, 2012, **487**(7405), 64–69, DOI: **10.1038/nature11220**.

25 Y. Sun, J. Sun, M. Xiao, W. Lai, L. Li, C. Fan and H. Pei, DNA Origami–Based Artificial Antigen-Presenting Cells for

Adoptive T Cell Therapy, *Sci. Adv.*, 2022, **8**(48), eadd1106, DOI: 10.1126/sciadv.add1106.

26 J. Hellmeier, R. Platzer, V. Mühlgrabner, M. C. Schneider, E. Kurz, G. J. Schütz, J. B. Huppa and E. Sevcsik, Strategies for the Site-Specific Decoration of DNA Origami Nanostructures with Functionally Intact Proteins, *ACS Nano*, 2021, **15**(9), 15057–15068, DOI: 10.1021/acsnano.1c05411.

27 H. Bila, K. Paloja, V. Caroprese, A. Kononenko and M. M. C. Bastings, Multivalent Pattern Recognition through Control of Nano-Spacing in Low-Valency Super-Selective Materials, *J. Am. Chem. Soc.*, 2022, **144**(47), 21576–21586, DOI: 10.1021/jacs.2c08529.

28 M. Zheng, Pathogen-Associated Geometric Patterns, *Colloids Surf. B Biointerfaces*, 2025, **245**, 114239, DOI: 10.1016/j.colsurfb.2024.114239.

29 F. L. Scott, B. Stec, C. Pop, M. K. Dobaczewska, J. J. Lee, E. Monosov, H. Robinson, G. S. Salvesen, R. Schwarzenbacher and S. J. Riedl, The Fas–FADD Death Domain Complex Structure Unravels Signalling by Receptor Clustering, *Nature*, 2009, **457**(7232), 1019–1022, DOI: 10.1038/nature07606.

30 L. Li, J. Yin, W. Ma, L. Tang, J. Zou, L. Yang, T. Du, Y. Zhao, L. Wang, Z. Yang, C. Fan, J. Chao and X. Chen, A DNA Origami Device Spatially Controls CD95 Signalling to Induce Immune Tolerance in Rheumatoid Arthritis, *Nat. Mater.*, 2024, **23**(7), 993–1001, DOI: 10.1038/s41563-024-01865-5.

31 C. A. Diebolder, F. J. Beurskens, R. N. de Jong, R. I. Koning, K. Strumane, M. A. Lindorfer, M. Voorhorst, D. Ugurlar, S. Rosati, A. J. R. Heck, J. G. J. van de Winkel, I. A. Wilson, A. J. Koster, R. P. Taylor, E. Ollmann Saphire, D. R. Burton, J. Schuurman, P. Gros and P. W. H. I. Parren, Complement Is Activated by IgG Hexamers Assembled at the Cell Surface, *Science*, 2014, **343**(6176), 1260–1263, DOI: 10.1126/science.1248943.

32 K. Paloja, J. Weiden, J. Hellmeier, A. S. Eklund, S. C. M. Reinhardt, I. A. Parish, R. Jungmann and M. M. C. Bastings, Balancing the Nanoscale Organization in Multivalent Materials for Functional Inhibition of the Programmed Death-1 Immune Checkpoint, *ACS Nano*, 2024, **18**(2), 1381–1395, DOI: 10.1021/acsnano.3c06552.

33 R. Veneziano, T. J. Moyer, M. B. Stone, E.-C. Wamhoff, B. J. Read, S. Mukherjee, T. R. Shepherd, J. Das, W. R. Schief, D. J. Irvine and M. Bathe, Role of Nanoscale Antigen Organization on B-Cell Activation Probed Using DNA Origami, *Nat. Nanotechnol.*, 2020, **15**(8), 716–723, DOI: 10.1038/s41565-020-0719-0.

34 F. Shen, Z. Xiong, Y. Wu, R. Peng, Y. Wang, L. Sun, C. Fan and Z. Liu, Precise Epitope Organization with Self-Adjuvant Framework Nucleic Acid for Efficient COVID-19 Peptide Vaccine Construction, *Angew. Chem., Int. Ed.*, 2023, **62**(21), e202301147, DOI: 10.1002/anie.202301147.

35 A. Comberlato, M. M. Koga, S. Nüssing, I. A. Parish and M. M. C. Bastings, Spatially Controlled Activation of Toll-like Receptor 9 with DNA-Based Nanomaterials, *Nano Lett.*, 2022, **22**(6), 2506–2513, DOI: 10.1021/acs.nanolett.2c00275.

36 R. M. L. Berger, J. M. Weck, S. M. Kempe, O. Hill, T. Liedl, J. O. Rädler, C. Monzel and A. Heuer-Jungemann, Nanoscale FasL Organization on DNA Origami to Decipher Apoptosis Signal Activation in Cells, *Small*, 2021, **17**(26), 2101678, DOI: 10.1002/smll.202101678.

37 M. Saitakis, S. Dogniaux, C. Goudot, N. Bufi, S. Asnacios, M. Maurin, C. Randriamampita, A. Asnacios and C. Hivroz, Different TCR-Induced T Lymphocyte Responses Are Potentiated by Stiffness with Variable Sensitivity, *eLife*, 2017, **6**, e23190, DOI: 10.7554/eLife.23190.

38 A. S. Eklund, A. Comberlato, I. A. Parish, R. Jungmann and M. M. C. Bastings, Quantification of Strand Accessibility in Biostable DNA Origami with Single-Staple Resolution, *ACS Nano*, 2021, **15**(11), 17668–17677, DOI: 10.1021/acsnano.1c05540.

39 K. Paloja, H. J. Rodríguez-Franco, R. Jungmann, I. A. Parish and M. M. C. Bastings, Multivalent Presentation of TCRs on DNA Nanostructures as a Sensitive Probe for pMHC Detection, *ACS Appl. Nano Mater.*, 2025, **8**(24), 12490–12497, DOI: 10.1021/acsanm.5c01296.

40 C.-H. Wang, X.-Q. Chen, Y.-Y. Su, H. Wang and D. Li, Precise Regulating T Cell Activation Signaling with Spatial Controllable Positioning of Receptors on DNA Origami, *Chin. J. Anal. Chem.*, 2022, **50**(6), 100091, DOI: 10.1016/j.cjac.2022.100091.

41 E. Sherman, V. Barr, S. Manley, G. Patterson, L. Balagopalan, I. Akpan, C. K. Regan, R. K. Merrill, C. L. Sommers, J. Lippincott-Schwartz and L. E. Samelson, Functional Nanoscale Organization of Signaling Molecules Downstream of the T Cell Antigen Receptor, *Immunity*, 2011, **35**(5), 705–720, DOI: 10.1016/j.immuni.2011.10.004.

42 M. J. Taylor, K. Husain, Z. J. Gartner, S. Mayor and R. D. Vale, A DNA-Based T Cell Receptor Reveals a Role for Receptor Clustering in Ligand Discrimination, *Cell*, 2017, **169**(1), 108–119, DOI: 10.1016/j.cell.2017.03.006.e20.

43 J. Goyette, D. J. Nieves, Y. Ma and K. Gaus, How Does T Cell Receptor Clustering Impact on Signal Transduction, *J. Cell Sci.*, 2019, **132**(4), jcs226423, DOI: 10.1242/jcs.226423.

44 A. Shaw, I. T. Hoffecker, I. Smyrlaki, J. Rosa, A. Grevys, D. Bratlie, I. Sandlie, T. E. Michaelsen, J. T. Andersen and B. Högberg, Binding to Nanopatterned Antigens Is Dominated by the Spatial Tolerance of Antibodies, *Nat. Nanotechnol.*, 2019, **14**(2), 184–190, DOI: 10.1038/s41565-018-0336-3.

45 P. Bousso and E. Robey, Dynamics of CD8+ T Cell Priming by Dendritic Cells in Intact Lymph Nodes, *Nat. Immunol.*, 2003, **4**(6), 579–585, DOI: 10.1038/ni928.

46 M. Cebecauer, P. Guillaume, P. Hozák, S. Mark, H. Everett, P. Schneider and I. F. Luescher, Soluble MHC-Peptide Complexes Induce Rapid Death of CD8+ CTL1, *J. Immunol.*, 2005, **174**(11), 6809–6819, DOI: 10.4049/jimmunol.174.11.6809.

47 M. A. Al-Aghbar, A. K. Jainarayanan, M. L. Dustin and S. R. Roffler, The Interplay between Membrane Topology and Mechanical Forces in Regulating T Cell Receptor Activity, *Commun. Biol.*, 2022, **5**(1), 1–16, DOI: 10.1038/s42003-021-02995-1.

48 K. Shah, A. Al-Haidari, J. Sun and J. U. Kazi, T Cell Receptor (TCR) Signaling in Health and Disease, *Signal Transduct. Target. Ther.*, 2021, **6**(1), 412, DOI: 10.1038/s41392-021-00823-w.

49 G. Gaud, R. Lesourne and P. E. Love, Regulatory Mechanisms in T Cell Receptor Signalling, *Nat. Rev. Immunol.*, 2018, **18**(8), 485–497, DOI: 10.1038/s41577-018-0020-8.

50 J. Oh, X. Xia, W. K. R. Wong, S. H. D. Wong, W. Yuan, H. Wang, C. H. N. Lai, Y. Tian, Y.-P. Ho, H. Zhang, Y. Zhang, G. Li, Y. Lin and L. Bian, The Effect of the Nanoparticle Shape on T Cell Activation, *Small*, 2022, **18**(36), 2107373, DOI: **10.1002/smll.202107373**.

51 T. Sugawara, T. Moriguchi, E. Nishida and Y. Takahama, Differential Roles of ERK and P38 MAP Kinase Pathways in Positive and Negative Selection of T Lymphocytes, *Immunity*, 1998, **9**(4), 565–574, DOI: **10.1016/S1074-7613(00)80639-1**.

52 C. Lacouture, B. Chaves, D. Guipouy, R. Houmadi, V. Duplan-Eche, S. Allart, N. Destainville and L. Dupré, LFA-1 Nanoclusters Integrate TCR Stimulation Strength to Tune T-Cell Cytotoxic Activity, *Nat. Commun.*, 2024, **15**(1), 407, DOI: **10.1038/s41467-024-44688-3**.

53 J. Yi, L. Balagopalan, T. Nguyen, K. M. McIntire and L. E. Samelson, TCR Microclusters Form Spatially Segregated Domains and Sequentially Assemble in Calcium-Dependent Kinetic Steps, *Nat. Commun.*, 2019, **10**(1), 277, DOI: **10.1038/s41467-018-08064-2**.

54 S. J. Davis and P. A. van der Merwe, The Kinetic-Segregation Model: TCR Triggering and Beyond, *Nat. Immunol.*, 2006, **7**(8), 803–809, DOI: **10.1038/ni1369**.

55 H. Cai, J. Muller, D. Depoil, V. Mayya, M. P. Sheetz, M. L. Dustin and S. J. Wind, Full Control of Ligand Positioning Reveals Spatial Thresholds for T Cell Receptor Triggering, *Nat. Nanotechnol.*, 2018, **13**(7), 610–617, DOI: **10.1038/s41565-018-0113-3**.

56 S.-P. Cordoba, K. Choudhuri, H. Zhang, M. Bridge, A. B. Basat, M. L. Dustin and P. A. van der Merwe, The Large Ectodomains of CD45 and CD148 Regulate Their Segregation from and Inhibition of Ligated T-Cell Receptor, *Blood*, 2013, **121**(21), 4295–4302, DOI: **10.1182/blood-2012-07-442251**.

57 Y. Du, Y. Lyu, J. Lin, C. Ma, Q. Zhang, Y. Zhang, L. Qiu and W. Tan, Membrane-Anchored DNA Nanojunctions Enable Closer Antigen-Presenting Cell–T-Cell Contact in Elevated T-Cell Receptor Triggering, *Nat. Nanotechnol.*, 2023, **18**(7), 818–827, DOI: **10.1038/s41565-023-01333-2**.

58 M. E. Birnbaum, J. L. Mendoza, D. K. Sethi, S. Dong, J. Glanville, J. Dobbins, E. Özkan, M. M. Davis, K. W. Wucherpfennig and K. C. Garcia, Deconstructing the Peptide-MHC Specificity of T Cell Recognition, *Cell*, 2014, **157**(5), 1073–1087, DOI: **10.1016/j.cell.2014.03.047**.

